Results in Physics 2 (2012) 14–21

Contents lists available at SciVerse ScienceDirect

Results in Physics

journal homepage: www.journals.elsevier.com/results-in-physics

Investigate the interaction between dark matter and dark energy

Jianbo Lu [a,*], Yabo Wu [a], Yongyi Jin [b], Yan Wang [a]

[a] Department of Physics, Liaoning Normal University, Dalian 116029, PR China
[b] China Criminal Police University, Shenyang, PR China

ARTICLE INFO

Article history:
Received 5 December 2011
Received in revised form 15 February 2012
Accepted 15 February 2012
Available online 28 February 2012

Keywords:
Accelerating universe
Interaction between dark sections
Observational constraint

ABSTRACT

In this paper we investigate the interaction between dark matter and dark energy by considering two different interacting scenarios, i.e. the cases of constant interaction function and variable interaction function. By fitting the current observational data to constrain the interacting models, it is found that the interacting strength is non-vanishing, but weak for the case of constant interaction function, and the interaction is not obvious for the case of variable interaction function. In addition, for seeing the influence from interaction we also investigate the evolutions of interaction function, effective state parameter for dark energy and energy density of dark matter. At last some geometrical quantities in the interacting scenarios are discussed.

Contents

1. Introduction

The observation of the supernovae of type Ia [1,2] provides the evidence that the universe is undergoing accelerated expansion. In theory, a popular interpretation for this phenomenon is that an unknown fluid with negative pressure, dubbed dark energy, is introduced in the universe in the framework of standard cosmology. Many dark energy models [3–22] have been investigated in the recent years from different points of view such as cosmological constant, the fields of theory, holographic theory, string theory, etc. Though the cosmological constant model is consistent with the current astronomy observations at 2σ confidence level, it suffers from the fine tuning and the coincidence problems. One of the solutions to alleviating the above two problems is to consider the interaction between the two dark sectors of dark energy and dark matter. Several forms of the interacting parameter Γ have been studied [23–33], such as $\Gamma = -\lambda\dot{\rho}_{de}$, $\Gamma = -\lambda H\rho_{de}$, and $\Gamma = -\lambda H(\rho_{dm} + \rho_{de})$. In this paper, using the current observational data we investigate the interaction between dark sections with a different method introduced in Ref. [34].

* Corresponding author.
E-mail address: lvjianbo819@163.com (J. Lu).

2211-3797
doi:10.1016/j.rinp.2012.02.001

2. Interacting dark model

Considering three equations of conservation for baryon, dark matter, and dark energy, respectively

$$\dot{\rho}_b + 3H(\rho_b + p_b) = 0, \tag{1}$$
$$\dot{\rho}_{dm} + 3H\gamma^e_{dm}\rho_{dm} = 0, \tag{2}$$
$$\dot{\rho}_{de} + 3H\gamma^e_{de}\rho_{de} = 0, \tag{3}$$

with the introduced effective barotropic indexes γ^e_i [34],

$$\gamma^e_{dm} = \gamma_{dm} + \frac{\gamma_{de}}{r} + \frac{\dot{\rho}_{de}}{3H\rho_{dm}}, \tag{4}$$

$$\gamma^e_{de} = \gamma_{de} + \gamma_{dm}r + \frac{\dot{\rho}_{dm}}{3H\rho_{de}}, \tag{5}$$

where $r = \rho_{dm}/\rho_{de}$ and $\gamma_i = \frac{p_i}{\rho_i} + 1$. When $\gamma^e_{dm} = \gamma_{dm}$ and $\gamma^e_{de} = \gamma_{de}$, Eqs. (2) and (3) are reduced to the non-interacting cases. In addition, for the introduced effective barotropic indexes γ^e_i and the parameter r, they have the relations:

$$(\gamma^e_{dm} - \gamma_{dm})r + (\gamma^e_{de} - \gamma_{de}) = 0, \tag{6}$$
$$\dot{r} = -3Hr(\gamma^e_{dm} - \gamma^e_{de}). \tag{7}$$

Considering that the effective barotropic index of dark energy is given by $\gamma^e_{de} = \gamma_{de} - F(r)$ [34] with $F(r)$ being a function of the energy density ratio r, one get,

$$\gamma^e_{dm} - \gamma^e_{de} = \gamma_{dm} - \gamma_{de} + F(r)\left(1 + \frac{1}{r}\right), \tag{8}$$

and the energy conservation Eqs. (2) and (3) become

$$\dot{\rho}_{dm} + 3H\rho_{dm}\gamma_{dm} = -3H\rho_{de}F(r), \tag{9}$$
$$\dot{\rho}_{de} + 3H\rho_{de}\gamma_{de} = 3H\rho_{de}F(r). \tag{10}$$

It is obvious that $F(r)$ can be dubbed as interaction function, which measures the strength of interaction. From Eqs. (9) and (10), we can see the energy transfer between dark energy and dark matter, and for $F(r) = 0$ Eqs. (9) and (10) reduce to the non-interacting cases for the energy conservation equation. In the following we consider two concrete forms of interaction function $F(r)$.

2.1. Interacting dark model with a constant interaction function F(r)

For calculation, following Ref. [34] we consider a concrete form of the constant function $F(r)$ as

$$F(r) = -\frac{r_\infty}{1 + r_\infty}(\gamma_{dm} - \gamma_{de}), \tag{11}$$

where γ_{dm} and γ_{de} are considered as constant, and the parameter r_∞ is also a constant which denotes the ratio between the energy densities at infinity. From Eq. (11) it is easy to see that for the parameter $r_\infty = 0$, the non-interacting energy conservation equations for dark matter and dark energy are obtained in Eqs. (9) and (10). Integrating Eqs. (7), (2), and (3), we get the expressions of the energy density for dark matter and dark energy,

$$\rho_{dm} = \rho_{0de}[r_\infty + (r_0 - r_\infty)(1+z)^{3\alpha}](1+z)^\beta, \tag{12}$$

$$\rho_{de} = \rho_{0de}(1+z)^\beta, \tag{13}$$

where r_0 denotes the current value of the parameter r, and two defined parameters,

$$\alpha = \frac{\gamma_{dm} - \gamma_{de}}{1 + r_\infty}, \tag{14}$$
$$\beta = 3\frac{r_\infty\gamma_{dm} + \gamma_{de}}{1 + r_\infty}. \tag{15}$$

Considering the definitions of the dimensionless energy densities, $\Omega_{0b} = \frac{8\pi G\rho_{0b}}{3H_0^2}$, $\Omega_{0dm} = \frac{8\pi G\rho_{0dm}}{3H_0^2}$ and $\Omega_{0de} = \frac{8\pi G\rho_{0de}}{3H_0^2}$, the Friedmann equation can be written as

$$\begin{aligned} E^2 &= \frac{H^2}{H_0^2} = \frac{8\pi G}{3H_0^2}(\rho_b + \rho_{dm} + \rho_{de}) \\ &= \Omega_{0b}(1+z)^3 + (1 - \Omega_{0b} - \Omega_{0de} - r_\infty\Omega_{0de})(1+z)^3 \\ &\quad + \Omega_{0de}(1 + r_\infty)(1+z)^\beta \\ &= \Omega_{0m}(1+z)^3 + (1 - \Omega_{0m})(1 + r_\infty)(1+z)^\beta - (1 \\ &\quad - \Omega_{0m})r_\infty(1+z)^3, \end{aligned} \tag{16}$$

with using the relation $\Omega_{0b} + \Omega_{0dm} + \Omega_{0de} = 1$.

2.2. Interacting dark model with a variable interaction function F(r)

In this part we consider a concrete variable interaction function $F(r)$ to investigate the interaction between dark matter and dark energy. Following Ref. [34], one possible choice for the function $F(r)$ is

$$F(r) = -\frac{(1-r)r_\infty^2}{r(1 - r_\infty^2)}(\gamma_{dm} - \gamma_{de}). \tag{17}$$

With using Eq. (17), integrating Eqs. (2) and (3) one can get the energy densities of dark matter and dark energy

$$\rho_{dm} = \rho_{0de}\sqrt{r_\infty^2 + (r_0^2 - r_\infty^2)(1+z)^\mu}(1+z)^{3v}\left[\frac{(1 - r/r_\infty)(1 + r_0/r_\infty)}{(1 - r_0/r_\infty)(1 + r/r_\infty)}\right]^{\frac{r_\infty}{2}}, \tag{18}$$

$$\rho_{de} = \rho_{0de}(1+z)^{3v}\left[\frac{(1 - r/r_\infty)(1 + r_0/r_\infty)}{(1 - r_0/r_\infty)(1 + r/r_\infty)}\right]^{\frac{r_\infty}{2}}, \tag{19}$$

where

$$\mu = \frac{6(\gamma_{dm} - \gamma_{de})}{1 - r_\infty^2}, v = \gamma_{de} - \frac{(\gamma_{dm} - \gamma_{de})r_\infty^2}{1 - r_\infty^2}. \tag{20}$$

So, the expression of dimensionless Hubble parameter can be written as

$$\begin{aligned} E(z)^2 &= \frac{H(z)^2}{H_0^2} \\ &= \Omega_{0de}(1+z)^{3v}\left[\frac{(1 - r/r_\infty)(1 + r_0/r_\infty)}{(1 - r_0/r_\infty)(1 + r/r_\infty)}\right]^{\frac{r_\infty}{2}} \\ &\quad \times \left[1 + \sqrt{r_\infty^2 + (r_0^2 - r_\infty^2)(1+z)^\mu}\right] + \Omega_{0b}(1+z)^3. \end{aligned} \tag{21}$$

For the above two interacting cases, according to Eqs. (16) and (21) one can see that they are reduced to the non-interacting case with a model-independent dark energy scenario $w = w_0 =$ constant, when the parameter $r_\infty = 0$.

3. Cosmological constraints on the interacting models of dark sectors

In the following we apply the current observational data to constrain the above interacting models of dark matter and dark energy. For the used observational data, we consider 557 Union2 dataset of type supernovae Ia (SNIa) [35], observational Hubble data (OHD) [36], X-ray gas mass fraction in cluster [37], baryon acoustic oscillation (BAO) [38], and cosmic microwave background (CMB) data [39].

3.1. Type Ia supernovae

For SNIa observation, distance modulus $\mu(z)$ is expressed as

$$\mu_{th}(z) = 5\log_{10}[D_L(z)] + \mu_0, \tag{22}$$

where $D_L(z) = H_0 d_L(z)/c$ is the Hubble-free luminosity distance, with H_0 being the Hubble constant defined by the re-normalized quantity h as $H_0 = 100\,h\ \mathrm{km\ s^{-1}\,Mpc^{-1}}$, and

$$d_L(z) = c(1+z)\int_0^z \frac{dz'}{H(z')},$$
$$\mu_0 = 5\log_{10}\left(\frac{H_0^{-1}}{Mpc}\right) + 25 = 42.38 - 5\log_{10}h,$$

for a flat-geometry universe. Additionally, the observed distance moduli $\mu_{obs}(z_i)$ of SNIa at z_i are

$$\mu_{obs}(z_i) = m_{obs}(z_i) - M, \tag{23}$$

where M is their absolute magnitudes.

For using SNIa data, theoretical model parameters θ can be determined by a likelihood analysis, based on the calculation of

$$\chi^2(\theta, M') \equiv \sum_{SNIa} \frac{\{\mu_{obs}(z_i) - \mu_{th}(\theta, z_i)\}^2}{\sigma_i^2} = \sum_{SNIa} \frac{\{5\log_{10}[D_L(\theta, z_i)] - m_{obs}(z_i) + M'\}^2}{\sigma_i^2}, \tag{24}$$

where $M' \equiv \mu_0 + M$ is a nuisance parameter which includes the absolute magnitude and the parameter h. The nuisance parameter M' can be marginalized over analytically [40–46] as

$$\bar{\chi}^2(\theta) = -2\ln\int_{-\infty}^{+\infty} \exp\left[-\frac{1}{2}\chi^2(\theta, M')\right] dM',$$

resulting to

$$\bar{\chi}^2 = A - \frac{B^2}{C} + \ln\left(\frac{C}{2\pi}\right), \tag{25}$$

with

$$A = \sum_{SNIa} \frac{\{5\log_{10}[D_L(\theta, z_i)] - m_{obs}(z_i)\}^2}{\sigma_i^2},$$
$$B = \sum_{SNIa} \frac{5\log_{10}[D_L(\theta, z_i)] - m_{obs}(z_i)}{\sigma_i^2},$$
$$C = \sum_{SNIa} \frac{1}{\sigma_i^2}.$$

Noting that the expression

$$\chi^2_{SNIa}(\theta) = A - (B^2/C),$$

which is equivalent to (25) except a constant, then it is often used in the likelihood analysis, since in this case the constraint results will not be affected by the nuisance parameter M'.

3.2. Observational Hubble data

The observational Hubble data [47] are based on differential ages of the galaxies. In [48], Jimenez et al. obtained an independent estimate for the Hubble parameter using the method developed in [49], and used it to constrain the cosmological models. The Hubble parameter depending on the differential ages as a function of redshift z can be written in the form of

$$H(z) = -\frac{1}{1+z}\frac{dz}{dt}. \tag{26}$$

So, once dz/dt is known, $H(z)$ is obtained directly. By using the differential ages of passively-evolving galaxies from the Gemini Deep Deep Survey (GDDS) [50] and archival data [51], Simon et al. obtained several values of $H(z)$ at different redshift [36]. The 12 observational Hubble data (redshift interval $0 \lesssim z \lesssim 1.8$) from [52–55] are listted in Table 1. In addition, in [55] the authors take the BAO scale as a standard ruler in the radial direction, and obtain three more additional data: $H(z = 0.24) = 79.69 \pm 2.32$, $H(z = 0.34) = 83.8 \pm 2.96$, and $H(z = 0.43) = 86.45 \pm 3.27$.

The best fit values of the model parameters from observational Hubble data are determined by minimizing [56–58]

$$\chi^2_{OHD}(H_0, \theta) = \sum_{i=1}^{15} \frac{[H_{th}(H_0, \theta; z_i) - H_{obs}(z_i)]^2}{\sigma^2(z_i)}, \tag{27}$$

where H_{th} is the predicted value for the Hubble parameter, H_{obs} is the observed value, $\sigma(z_i)$ is the standard deviation measurement uncertainty, and the summation is over the 15 observational Hubble data points at redshifts z_i.

3.3. The X-ray gas mass fraction

The observations of X-ray gas mass fraction in galaxy clusters provide the information on the dark matter and the formation of structure, so they can be used to constrain the cosmological parameters. It is assumed that the baryon gas mass fraction in clusters [59]

$$f_{gas} = \frac{M_{b-gas}}{M_{tot}} \tag{28}$$

is constant, independent of redshift and is related to the global fraction of the universe Ω_b/Ω_{0m}. In the standard cold dark matter (SCDM) model, f_{gas}^{SCDM} is [59]

$$f_{gas}^{SCDM} = \frac{b}{1+\alpha}\frac{\Omega_b}{\Omega_{0m}}\left(\frac{d_A^{SCDM}(z)}{d_A(z)}\right)^{\frac{3}{2}}, \tag{29}$$

where d_A is diameter distance which relates with d_L via $d_L(z) = (1+z)^2 d_A(z)$, the parameter b is a bias factor suggesting that the baryon fraction in clusters is slightly lower than for the universe as a whole, the parameter $\alpha \simeq 0.19\sqrt{h}$ is the ratio factor of optically luminous baryonic mass with X-ray gas contained in clusters. From Cluster Baryon Fraction (CBF), the best fit values of parameters in cosmological model can be determined by minimizing [59]

$$\chi^2_{CBF}(\theta) = C - \frac{B^2}{A}, \tag{30}$$

Table 1
The observational $H(z)$ data [52–55].

z	0	0.1	0.17	0.27	0.4	0.48	0.88	0.9	1.30	1.43	1.53	1.75
$H(z)$ ($\mathrm{km\ s^{-1}\ Mpc^{-1}}$)	74.2	69	83	77	95	97	90	117	168	177	140	202
1σ Uncertainty	±3.6	±12	±8	± 14	±17	±60	±40	±23	±17	±18	±14	±40

where

$$A=\sum_{i=1}^{N}\frac{\tilde{f}_{gas}^{SCDM}(z_i)^2}{\sigma_{f_{gas,i}}^2},$$
$$B=\sum_{i=1}^{N}\frac{\tilde{f}_{gas}^{SCDM}(z_i)\cdot f_{gas,i}}{\sigma_{f_{gas,i}}^2}, \quad (31)$$
$$C=\sum_{i=1}^{N}\frac{f_{gas,i}^2}{\sigma_{f_{gas,i}}^2},$$

and

$$\tilde{f}_{gas}^{SCDM}(z_i)=\left(\frac{d_A^{SCDM}(z)}{d_A(z)}\right)^{\frac{3}{2}}. \quad (32)$$

$N = 42$ is the number of the observed $f_{gas,i}$ and $\sigma_{gas,i}^2$ published in Ref. [60].

3.4. Baryon acoustic oscillation

The baryon acoustic oscillations are detected in the clustering of the 2dFGRS and SDSS main galaxy samples, which measure the distance-redshift relation. The value of dimensionless parameter A can be calculated from these samples, which is defined by

$$A=\sqrt{\Omega_{0m}}E(z_{BAO})^{-1/3}\left[\frac{1}{z_{BAO}}\int_0^z\frac{dz'}{E(z';\theta)}\right]^{2/3}, \quad (33)$$

where $E(z)$ is included in the Hubble parameter $H(z) = H_0E(z)$, and the values of $z_{BAO} = 0.35$ and $A = 0.469 \pm 0.017$ are given by measuring from the SDSS [61–63]. One can minimize the χ_{BAO}^2 defined as

$$\chi_{BAO}^2(\theta)=\frac{(A(\theta)-0.469)^2}{0.017^2}. \quad (34)$$

3.5. Cosmic microwave background

For CMB data, we use the CMB shift parameter R to constrain the cosmological model. It is defined by [64]

$$R=\sqrt{\Omega_{0m}H_0^2}(1+z_*)D_A(z_*)/c=\sqrt{\Omega_m}\int_0^{z_*}\frac{H_0dz'}{H(z';\theta)}, \quad (35)$$

here z_* is the redshift at the decoupling epoch of photons, which is obtained from the 7yWMAP data $z_* = 1091.3$, and the value of R is given by [39]

$$R=1.725\pm0.018. \quad (36)$$

From the CMB constraint, the best fit values of parameters in the DE models can be determined by minimizing

$$\chi_{CMB}^2(\theta)=\frac{(R(\theta)-1.725)^2}{0.018^2}. \quad (37)$$

The total χ^2 is expressed as

$$\chi_{total}^2(\theta)=\sum_i\chi_i^2(\theta), \quad (38)$$

here θ denotes the model parameters, and suffix i denotes any one observational data of the above five data: SNIa, OHD, CBF, BAO and CMB. In this expression, for each observation χ^2 corresponds to Eqs. (26), (27), (30), (34) and (37), respectively. Using the currently observed data, Figs. 1–3 respectively plot the 2-D contours with 1σ,2σ confidence levels of model parameters in the flat universe for the case of $F(r)$ = constant, $F(r)$ = variable and non-interacting model of $w = w_0$ = constant. And for each model we consider three different combined constraints on model parameters, i.e. respectively using the combined data of SNIa + OHD + BAO, SNIa + CMB and SNIa + OHD + CBF + BAO + CMB. The corresponding calculation results for the constraints on model parameters are listed in Tables 2–4. According to these three constraints on the parameter r_∞, as shown in Table 2 one can see that for the case of the constant interaction function $F(r)$, there exists a non-vanishing, but weak interaction. However, for the case of the variable interaction function $F(r)$, considering that the best fit values of r_∞ are near to zero it seems that the observational data tend to have no interaction between dark matter and dark energy, but the confidence levels of this parameter are still wide. Also, from Tables 2–4 it can be seen that the most stringent constraint on model parameters is given by using the most observational data: SNIa + OHD + CBF + BAO + CMB, when compare three combined constraints. In addition, by using

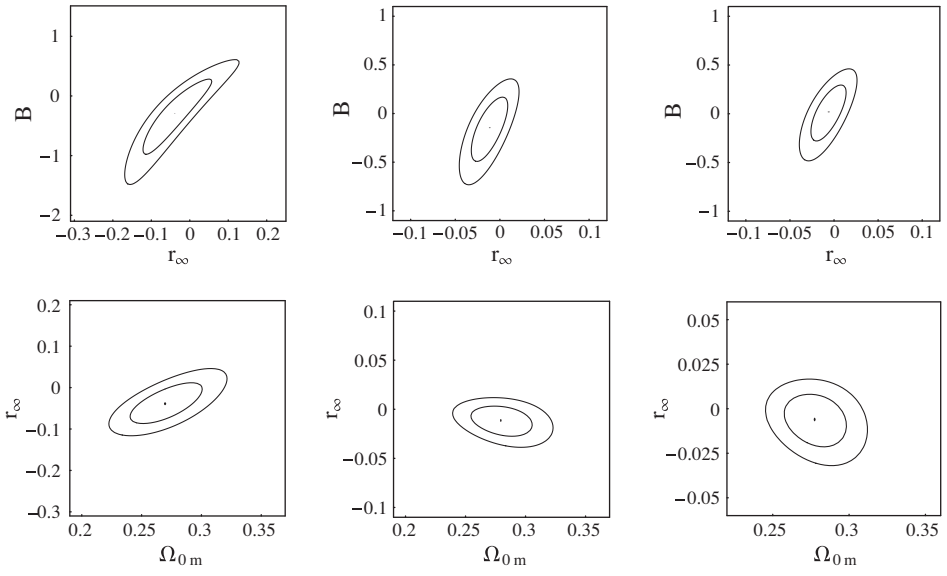

Fig. 1. The 2-D contours with 1σ and 2σ confidence levels of model parameters in the interacting model with considering a constant function $F(r)$ from the current observational data: SNIa + OHD + BAO (left), SNIa + CMB (middle) and SNIa + OHD + CBF + BAO + CMB (right).

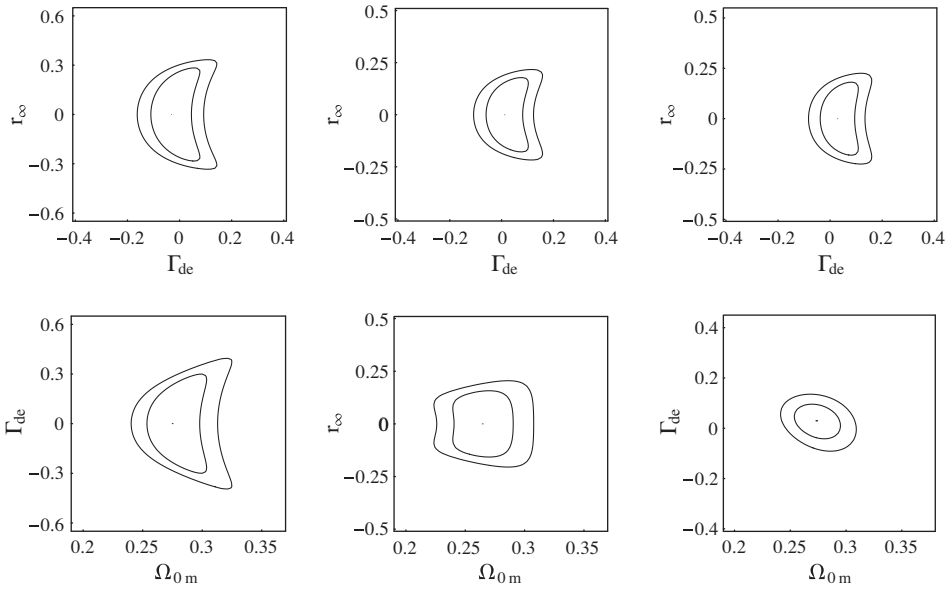

Fig. 2. The 2-D contours with 1σ and 2σ confidence levels of model parameters in the interacting model with considering a variable function $F(r)$ by using SNIa + OHD + BAO (left), SNIa + CMB (middle) and SNIa + OHD + CBF + BAO + CMB data (right).

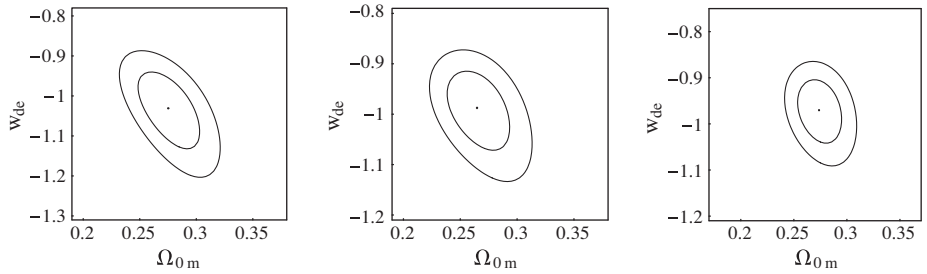

Fig. 3. The 2-D contours with 1σ and 2σ confidence levels of model parameters in the non-interacting model of $w = w_0 =$ constant by using SNIa + OHD + BAO (left), SNIa + CMB (middle) and SNIa + OHD + CBF + BAO + CMB data (right).

Table 2
The values of χ^2_{min}, χ^2_{min}/dof, and the best fit values of model parameters with their confidence levels for the constant interacting model from the current observational data: SNIa + OHD + BAO, SNIa + CMB and SNIa + OHD + CBF + BAO + CMB, where the value of *dof* (degree of freedom) equals the number of observational data points minus the number of model parameters.

	χ^2_{min}	χ^2_{min}/dof	Ω_{0m}	r_∞	β
SNIa + OHD + BAO	554.092	0.967	$0.270^{+0.033+0.053}_{-0.032-0.049}$	$-0.039^{+0.096+0.167}_{-0.083-0.122}$	$-0.295^{+0.577+0.904}_{-0.682-1.189}$
SNIa + CMB	542.633	0.972	$0.279^{+0.029+0.046}_{-0.026-0.042}$	$-0.011^{+0.020+0.032}_{-0.021-0.033}$	$-0.146^{+0.315+0.502}_{-0.346-0.586}$
SNIa + OHD + CBF + BAO + CMB	616.397	1.001	$0.277^{+0.023+0.037}_{-0.021-0.034}$	$-0.006^{+0.020+0.032}_{-0.020-0.033}$	$0.019^{+0.275+0.442}_{-0.298-0.492}$

Table 3
The values of χ^2_{min}, χ^2_{min}/dof, and the best fit values of model parameters with their confidence levels for the variable interacting model from the current observational data.

	χ^2_{min}	χ^2_{min}/dof	Ω_{0m}	r_∞	γ_{de}
SNIa + OHD + BAO	554.41	0.968	$0.275^{+0.031+0.052}_{-0.023-0.037}$	$-0.00001^{+0.586+0.919}_{-0.692-1.211}$	$-0.031^{+0.091+0.158}_{-0.077-0.121}$
SNIa + CMB	542.73	0.973	$0.265^{+0.027+0.045}_{-0.028-0.043}$	$-0.0005^{+0.1788+0.2175}_{-0.1778-0.2165}$	$0.012^{+0.091+0.146}_{-0.072-0.120}$
SNIa + OHD + CBF + BAO + CMB	616.537	1.001	$0.274^{+0.023+0.037}_{-0.022-0.035}$	$-0.00004^{+0.18147+0.22541}_{-0.18139-0.22526}$	$0.030^{+0.078+0.130}_{-0.068-0.113}$

the best fit values of model parameters we can obtain the values of state parameter for dark energy w_{de}, according to the calculation formula $w_{de} = \gamma_{de} - 1 = \frac{\beta(1+r_\infty)}{3} - r_\infty\gamma_{dm} - 1$ for the case of constant interaction function, and$w_{de} = \gamma_{de} - 1$ for the case of variable interaction function. It is shown that for both interacting scenarios, the values of state parameter w_{de} are in phantom region ($w_{de} < -1$) for the combined constraint from SNIa + OHD + BAO data, and are in quintessence region ($w_{de} > -1$) for the combined constraint from SNIa + OHD + CBF + BAO + CMB data, which are consistent with the constraint results of the non-interacting case.

In addition, for seeing the influence from the interaction function we also plot the evolutions of the effective state parameter

Table 4
The values of χ^2_{min}, χ^2_{min}/dof, and the best fit values of model parameters with their confidence levels for the non-interacting model from the current observational data.

	χ^2_{min}	χ^2_{min}/dof	Ω_{0m}	w_0
SNIa + OHD + BAO	554.410	0.968	$0.275^{+0.028+0.046}_{-0.027-0.043}$	$-1.031^{+0.091+0.144}_{-0.101-0.172}$
SNIa + CMB	542.730	0.973	$0.265^{+0.028+0.048}_{-0.026-0.042}$	$-0.988^{+0.073+0.116}_{-0.084-0.145}$
SNIa + OHD + CBF + BAO + CMB	616.537	1.001	$0.274^{+0.021+0.035}_{-0.020-0.033}$	$-0.970^{+0.066+0.106}_{-0.072-0.121}$

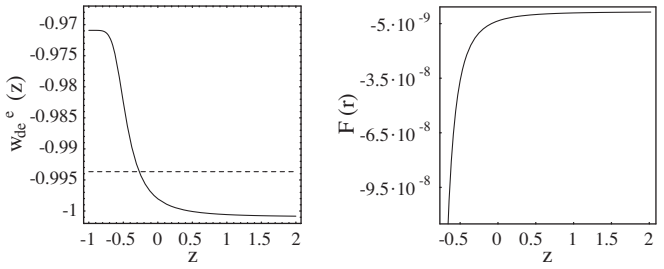

Fig. 4. The evolutions of the effective state parameter for dark energy $w^e_{de}(z)$ (left) in interacting model with constant function $F(r)$ (dot line) and variable function $F(r)$ (solid line), and the evolution of variable interactioin function $F(r)$ (right).

for dark energy $w^e_{de} = \gamma^e_{de} - 1$ and the interaction function $F(r)$. The effective state parameter for dark energy in the above two interacting scenarios are respectively expressed as

$$\begin{aligned} w^e_{de} &= \gamma^e_{de} - 1 = \gamma_{de} + r\gamma_{dm} + \frac{\dot{\rho}_{dm}}{3H\rho_{de}} - 1 \\ &= -1 + \gamma_{de} + \left(\gamma_{dm} - \frac{\beta}{3}\right)[r_\infty + (r_0 - r_\infty)(1+z)^{\frac{3(\gamma_{dm}-\gamma_{de})}{1+r_\infty}}] \\ &\quad - \frac{\gamma_{dm} - \gamma_{de}}{1+r_\infty}(r_0 - r_\infty)(1+z)^{\frac{3(\gamma_{dm}-\gamma_{de})}{1+r_\infty}} \end{aligned} \tag{39}$$

for the interacting model with a constant function $F(r)$, and

$$\begin{aligned} w^e_{de} &= -1 + \gamma_{de} - \frac{r^2_\infty \mu}{6} + (\gamma_{dm} - \nu)\sqrt{r^2_\infty + (r^2_0 - r^2_\infty)(1+z)^\mu} \\ &\quad - \frac{\mu(r^2_0 - r^2_\infty)(1+z)^\mu}{6\sqrt{r^2_\infty + (r^2_0 - r^2_\infty)(1+z)^\mu}} \end{aligned} \tag{40}$$

for the interacting model with a variable function $F(r)$. By using the best fit values of model parameters from the combined constraint of SNIa + OHD + CBF + BAO + CMB data, where $r_\infty = -0.006$ and $\gamma_{de} = 0.012$, the evolutions of effective state parameter for dark energy $w^e_{de}(z)$ in above two interacting scenarios are plotted in Fig. 4 (left). From this figure one can see that for the case of constant interaction function, the $w^e_{de}(z)$ is almost constant; and for the case of variable interaction function, the parameter $w^e_{de}(z)$ slowly change with respect to the redshift z. Furthermore for the interaction function $F(r)$, we have the best fit value of $F(r) = -\frac{r_\infty}{1+r_\infty}(\gamma_{dm} - \gamma_{de}) = 0.006$ for the constant interacting case, and plot the best fit evolution of $F(r) = -\frac{(1-r)r^2_\infty}{r(1-r^2_\infty)}(\gamma_{dm} - \gamma_{de})$ in Fig. 4 (right) for the variable interaction function. From Fig. 4 (right) it is easy to see that the interaction between dark matter and dark energy is always very weak, though it is variational with respect to redshift z.

4. The evolutions of geometrical quantities with their confidence level

In this part we investigate the evolutions of some geometrical quantities with their confidence level, such as deceleration parameter $q(z)$ and jerk parameter $j(z)$. The confidence level on a function $f = f(\theta)$ in terms of the variables θ are calculated by

$$\sigma^2_f = \sum_i^m \left(\frac{\partial f}{\partial \theta_i}\right)^2 C_{ii} + 2\sum_i^m \sum_{j=i+1}^m \left(\frac{\partial f}{\partial \theta_i}\right)\left(\frac{\partial f}{\partial \theta_j}\right) C_{ij}, \tag{41}$$

where m is the number of parameters, θ denotes model parameters, C_{ij} is the covariance matrix of the fitting parameters that is the inverse of the Fisher matrix $\left(C^{-1}_{ij}\right) = \frac{1}{2}\frac{\partial^2 \chi^2(\theta)}{\partial\theta_i \partial\theta_j}$, $f(z;\theta_i)$ express any one cosmological parameter. The evolution of any cosmological quantity $f(z)$ with confidence level is given by

$$f_{1\sigma}(z) = f(z)|_{\theta=\bar{\theta}} \pm \sigma_f, \tag{42}$$

here $\bar{\theta}$ is the best fit values of the constraint parameters.

The deceleration parameter is defined as

$$q(z) \equiv -\frac{\ddot{a}}{aH^2} = (1+z)\frac{1}{H}\frac{dH}{dz} - 1. \tag{43}$$

For the case of constant interaction function $F(r)$, one has

$$\begin{aligned} q(z) &= -1 \\ &\quad + \frac{-3r_\infty(1-\Omega_{0m})(1+z)^3 + 3\Omega_{0m}(1+z)^3 + \beta(1+r_\infty)(1-\Omega_{0m})(1+z)^\beta}{2[-r_\infty(1-\Omega_{0m})(1+z)^3 + \Omega_{0m}(1+z)^3 + (1+r_\infty)(1-\Omega_{0m})(1+z)^\beta]}. \end{aligned} \tag{44}$$

For $r_\infty = 0$, it reduces to the non-interacting case. For the case of variable interaction function $F(r)$, the concrete form of deceleration parameter is not listed here, since this expression is too complex. In Fig. 5 we plot the evolutions of $q(z)$ for two interacting cases. According to the figures the calculation results for transition redshift z_T and current deceleration parameter q_0 are listed in Table 5. From Table 5, comparing two interacting scenarios it can been seen that the constant interacting model tends to have the smaller values of transition redshift z_T and the more violent decelerated-expansion rhythm at present (reflected by the smaller value of q_0). And from Fig. 5, it is easy to see that for the case of interacting model with a variable function $F(r)$, it has the more stringent constraints on the evolutions of deceleration parameter than the case of interacting model with a constant function $F(r)$.

The jerk parameter is defined by scale factor a and its third derivative [65–67],

$$j \equiv -\frac{1}{H^3}\left(\frac{\dddot{a}}{a}\right) = -\left[\frac{1}{2}(1+z)^2\frac{[H(z)^2]''}{H(z)^2} - (1+z)\frac{[H(z)^2]'}{H(z)^2} + 1\right]. \tag{45}$$

The use of the cosmic jerk parameter provides more parameter space for geometrical studies, and transitions between phases of different cosmic acceleration are more naturally described by models incorporating a cosmic jerk. Also, we list the expression of jerk parameter for the case of constant interaction function $F(r)$, with having a form

$$\begin{aligned} j &= -1 \\ &\quad - \frac{\beta(\beta-3)(1+r_\infty)(1-\Omega_{0m})(1+z)^\beta}{2[-r_\infty(1-\Omega_{0m})(1+z)^3 + \Omega_{0m}(1+z)^3 + (1+r_\infty)(1-\Omega_{0m})(1+z)^\beta]}. \end{aligned} \tag{46}$$

For the evolutions of jerk parameter $j(z)$ in interacting models including the cases of constant function and variable function are plotted in Fig. 6 by using the combined observational data of SNIa + OHD + CBF + BAO + CMB. The current values of jerk parame-

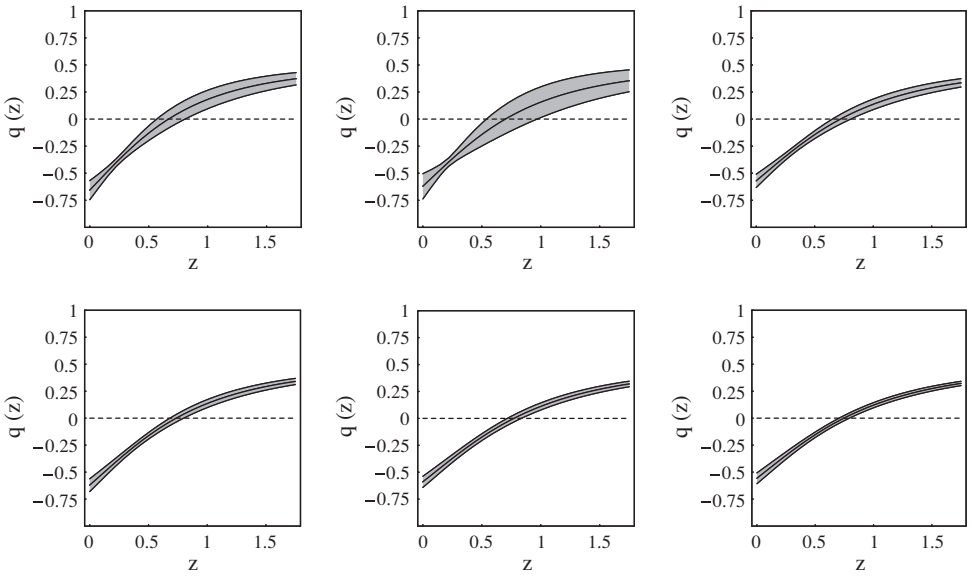

Fig. 5. The evolutions of $q(z)$ for interacting model with constant function $F(r)$ (upper) and variable function $F(r)$ (down), from the combined observational data of SNIa + OHD + BAO (left), SNIa + CMB (middle) and SNIa + OHD + CBF + BAO + CMB (right).

Table 5
The values of transition redshift z_T and current deceleration parameter q_0 for the interacting model with the constant function $F(r)$ (left) and the variable function $F(r)$ (right).

	z_T	q_0	z_T	q_0
SNIa + OHD + BAO	$0.669^{+0.137}_{-0.101}$	$-0.657^{+0.088}_{-0.087}$	$0.737^{+0.061}_{-0.054}$	$-0.621^{+0.059}_{-0.059}$
SNIa + CMB	$0.701^{+0.267}_{-0.162}$	$-0.621^{+0.166}_{-0.166}$	$0.773^{+0.060}_{-0.056}$	$-0.589^{+0.051}_{-0.052}$
SNIa + OHD + CBF + BAO + CMB	$0.721^{+0.085}_{-0.070}$	$-0.571^{+0.061}_{-0.060}$	$0.747^{+0.044}_{-0.042}$	$-0.557^{+0.050}_{-0.050}$

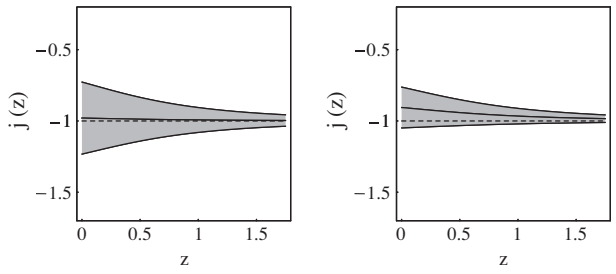

Fig. 6. The evolution of jerk parameter $j(z)$ for interacting model with constant function $F(r)$ (left) and variable function $F(r)$ (right) from the combined data: SNIa + OHD + CBF + BAO + CMB.

ter for the cases of constant and variable interaction function are respectively given by, $j_{01} = -0.980^{+0.253}_{-0.252}$ and $j_{02} = -0.906^{+0.156}_{-0.143}$. For the case of the non-interacting model-independent scenario, the evolutions of deceleration parameter $q(z)$ and jerk parameter $j(z)$, and the detailed discussions on the current values of deceleration parameter q_0 and jerk parameter j_0 can be found in Ref. [68], where the combined constraint results are obtained from the latest observational data, according to the analysis of Cosmography.

5. Conclusions

One knows the popular interpretation to the accelerating universe is the cosmological constant model. But this model suffers from the fine-tinning and the coincidence problems. And one of the solutions to solve these problems is to consider the interaction between two dark sections. In this paper, following Ref. [34] we investigate the interaction with using two different methods. We apply the current observed data, including 557 Union2 SNIa, OHD, cluster X-ray gas mass fraction, BAO and CMB data, to constrain the interacting dark models with considering the constant interaction function and the variable interaction function $F(r)$. According to the constraint results on model parameters, it indicates that the interaction between dark matter and dark energy is occurred, but the interacting strength is weak for the case of the constant function $F(r)$. When considering the interaction with the variable function, it seems that the interaction between dark matter and dark energy is not obvious for the best fit analysis. In addition, we consider the evolution of geometrical quantities, such as deceleration parameter and jerk parameter. It is shown that the most stringent constraint on deceleration parameter is given by the combined constraint of SNIa + OHD + CBF + BAO + CMB data. And we also get the constraint results on some cosmological quantities, such as transition redshift, current deceleration parameter and jerk parameter.

For the analysis of effective state parameter for dark energy w^e_{de} and dark-matter energy density ρ_{dm}, we consider using the best fit model parameters from the combined constraint of SNIa + OHD + CBF + BAO + CMB data. From Fig. 4 (left) it is shown that for the case of the variable interaction function, due to the influence of interaction between dark matter and dark energy the parameter w^e_{de} is dynamical, but the evolution is slow in the future ($z < 0$), and go near to be constant in the past ($z > 0$). For the case of the variable interaction function, w^e_{de} is almost constant all the time. Furthermore according to the best fit values of parameters $\alpha = \frac{(\gamma_{dm}-\gamma_{de})}{1+r_\infty} \simeq 0.982$ and $\beta = 3\frac{r_\infty\gamma_{dm}+\gamma_{de}}{1+r_\infty} \simeq 0.019$ for the constant interacting model, $\mu = \frac{6(\gamma_{dm}-\gamma_{de})}{1-r^2_\infty} \simeq 5.820$ and $\nu = \gamma_{de} - \frac{r^2_\infty(\gamma_{dm}-\gamma_{de})}{1-r^2_\infty}$ $\simeq 0.030$ for the variable interacting model, from Eqs. (12) and

(18) it can be found that for these two interacting models the evolutions of dark matter obey, $\rho_{dm1} \propto a^{-3\alpha-\beta} \simeq a^{-3.003}$ and $\rho_{dm2} \propto a^{-\mu/2+3\nu} \simeq a^{-3}$, which is similar to the popular understanding $\rho_{dm} \propto a^{-3}$. Then the acceleration-expanded universe will not appear in the matter-dominated phase for the interacting models (as shown in Fig. 5 about the evolution of deceleration parameter q), which is a fundamental for the structure formation. In addition, we note that according to the second law of thermodynamics [69], it requires that the energy density is transferred from dark energy to dark matter. From the analysis of interaction function, it is shown that $F(r)$ should be smaller than zero. This condition is satisfied for the case of variable interaction function (one can see in Fig. 4 (right)). For the case of constant interaction function, though the best fit value of $F(r)$ is not satisfied (since $r_{\infty} < 0$), it comes into existence at 1σ and 2σ confidence levels.

Acknowledgments

The research work is supported by the National Natural Science Foundation of China (11147150), the Natural Science Foundation of Education Department of Liaoning Province (L2011189), the Natural Science Foundation of Liaoning Province (Grant No. 20102124), the NSFC (11175077) and the NSFC (11005088) of PR China.

References

[1] Riess AG et al. Astron J 1998;116:1009.
[2] Perlmutter S et al. Astrophys J 1999;517:565.
[3] Ratra B, Peebels PJE. Phys Rev D 1988;37:3406.
[4] Feng B, Wang XL, Zhang XM. Phys Lett B 2005;607:35.
[5] Li M. Phys Lett B 2004;603:1.
[6] Cai RG. Phys Lett B 2007;657:228.
[7] Lu JB et al. Gen Rel Grav 2011;43:819–32.
[8] Wang YT, Xu LX. Phys Rev D 2010;81:083523.
[9] Kamenshchik AY, Moschella U, Pasquier V. Phys Lett B 2001;511:265.
[10] Lu JB et al. Phys Lett B 2008;662:87.
[11] Zhu ZH. Astron Astrophys 2004;423:421.
[12] Wu PX, Yu HW. Phys Lett B 2007;644:16.
[13] Gong YG. Phys Rev D 2000;61:043505.
[14] Gong YG. Phys Rev D 2000;61:043505.
[15] Gao C, Wu F, Chen X, Shen YG. Phys Rev D 2009;79:043511. arXiv:0712.1394.
[16] Lu JB, Saridakis EN, Setare MR, Xu LX. JCAP 2010;03:031.
[17] Lu JB, Xu LX, Liu ML, Gui YX. Eur Phys J C 2008;58:311.
[18] Lu JB, Xu LX. Int J Mod Phys D 2009;18:1741.
[19] Lu JB. Phys Lett B 2009;680:404.
[20] Feng CJ. Phys Lett B 2008;670:231–4.
[21] Lu JB et al. Eur Phys J Plus 2011;126:92.
[22] Lu JB et al. Eur Phys J C 2011;71:800.
[23] Zimdahl W, Pavon D. Phys Lett B 2001;521:133.
[24] Chimento LP, Jakubi AS, Pavon D, Zimdahl W. Phys Rev D 2003;67:083513.
[25] Feng C, Wang B, Abdalla E, Su R-K. Phys Lett B 2008;665:111.
[26] He JH, Wang B, Abdalla E. Phys Lett B 2009;671:139.
[27] Wang B, Zang J, Lin CY, Abdalla E, Micheletti S. Nucl Phys B 2007;778:69.
[28] Wang B, Gong YG, Abdalla E. Phys Lett B 2005;624:141.
[29] Cui J, Zhang X. Phys Lett B 2010;690:233–8.
[30] Abdalla E, Wang B. Phys Lett B 2007;651:89.
[31] Jamil M, Rashid MA. Eur Phys J 2008;C56:429.
[32] Bertolami O, Pedro FG, Delliou ML. Gen Rel Grav 2009;41:2839.
[33] Bertolami O, Gil Pedro F, Le Delliou M. Phys Lett B 2007;654:165.
[34] Chimento LP, Forte M, Kremer GM. Gen Rel Grav 2009;41:1125–37.
[35] R. Amanullah et al. [Supernova Cosmology Project Collaboration], [arXiv:astro-ph/1004.1711].
[36] Simon J, Verde L, Jimenez R. Phys Rev D 2005;71:123001.
[37] Allen SW, Rapetti DA, Schmidt RW, et al. Mon Not Roy Astron Soc 2008;383:879.
[38] W.J. Percival et al., [arXiv:astro-ph/0907.1660].
[39] E. Komatsu et al., [arXiv:astro-ph/1001.4538].
[40] Nesseris S, Perivolaropoulos L. Phys Rev D 2005;72:123519.
[41] Perivolaropoulos L. Phys Rev D 2005;71:063503.
[42] Acquaviva V, Verde L. JCAP 2007;0712:001.
[43] Guimaraes ACC, Cunha JV, Lima JAS. JCAP 2009;0910:010.
[44] Szydlowski M, Godlowski W. Phys Lett B 2006;633:427.
[45] Gannouji R, Polarski D. JCAP 2008;0805:018.
[46] Alam U, Sahni V. Phys Rev D 2006;73:084024.
[47] Yi ZL, Zhang TJ. Mod Phys Lett A 2007;22:41–53.
[48] Jimenez R, Verde L, Treu T, Stern D. Astrophys J 2003;593:622.
[49] Jimenez R, Loeb A. Astrophys J 2002;573:37.
[50] Abraham RG et al. Astron J 2004;127:2455.
[51] Nolan LA, Dunlop JS, Jimenez R, Heavens AF. Mon Not Roy Astron Soc 2003;341:464.
[52] D. Stern, R. Jimenez, L. Verde, M. Kamionkowski and S. A. Stanford, [arXiv:astro-ph/0907.3149].
[53] Simon J et al. Phys Rev D 2005;71:123001.
[54] A.G. Riess et al., arXiv:0905.0695[astro-ph].
[55] E. Gaztanñaga, A. Cabré and L. Hui, [arXiv:0807.3551].
[56] Lazkoz R, Majerotto E. JCAP 2007;0707:015.
[57] Samushia L, Ratra B. Astrophys J 2006;650:L5.
[58] Jimenez R, Verde L, Treu T, Stern D. Astrophys J 2003;593:622.
[59] Nesseris S, Perivolaropoulos L. JCAP 2007;0701:018.
[60] Allen SW, Rapetti DA, Schmidt RW, et al. Mon Not Roy Astron Soc 2008;383:879.
[61] Eisenstein DJ et al. Astrophys J 2005;633:560.
[62] Percival WJ et al. Mon Not Roy Astron Soc 2007;381:1053.
[63] Lu JB, Xu LX. Mod Phys Lett A 2010;25:737–47.
[64] Bond JR, Efstathiou G, Tegmark M. Mon Not Roy Astron Soc 1997;291:L33.
[65] Blandford RD. Mon Not Roy Astron Soc 2007;375:1510.
[66] X Xu L, Li WB, Lu JB. JCAP 2009;07:031.
[67] Lu JB, Xu LX, Liu ML. Phys Lett B 2011;699:246–50.
[68] Capozziello S, Lazkoz R, Salzano V. Phys Rev D 2011;84:124061.
[69] Pavon D, Wang B. Gen Rel Grav 2009;41:1.